

WP12

Theoretical Methods for Condensed Matter

Part II

Tom Frömbgen

Assistants: Sarah Löffelsender & Marcel Stahn

Submission 1: December 15, 2021

Submission 2: January 12, 2022

1 Partitioning Noncovalent Interactions

The interactions in weakly bound dimers were investigated using the symmetry-adapted perturbation theory^[1] (SAPT) as implemented in the MOLPRO2012 program package.^[2] By using the SAPT ansatz, the first and second order contributions to the complexation energy can be obtained as

$$E_{\text{SAPT}} = E_{\text{pol}} + E_{\text{exch}} + E_{\text{ind}} + E_{\text{exch-ind}} + E_{\text{disp}} + E_{\text{exch-disp}} . \quad (1)$$

A monomer description via HF or DFT is required.

1.1 Interactions in the argon, water and uracil dimers

Here, the interactions in the argon, water and uracil dimers were calculated and partitioned on the HF-SAPT/aug-cc-pVTZ^[3,4] and AC-PBE0^[5]/aug-cc-pVTZ level of theory. In case of PBE0, an asymptotic correction (AC) to the monomer exchange-correlation potential was added to obtain reasonable results. This DFT-based SAPT needs experimental and theoretical ionization energies as input for the dimer calculation to asymptotically correct the exchange-correlation functional. The experimental ones were obtained from the NIST webpage.^[6] For the theoretical ones a monomer calculation was performed, subsequently using the HOMO energy and the negative ionization potential according to Koopman's theorem. For the uracil dimer a smaller aug-cc-pVDZ basis set was used to reduce the computational effort. This was necessary because the used method scale with the fifth power of the molecular size and with the third power upon increase of the basis set size for a given dimer.^[7] Note that with the decreasing basis set size larger basis set incompleteness errors (BSIE) arise. It is important to mention that within the SAPT ansatz, there is per definition no basis set superposition error (BSSE) since no calculation of the full dimer is carried out.

The obtained energies are displayed in Table 1. The first order polarization energy E_{pol}^1 as well as the second order induction E_{ind}^2 and dispersion E_{disp}^2 energies are negative throughout all investigated dimers. This is reasonable since these processes are per definition attractive. Opposed to that, all exchange energies, E_{exch}^1 , $E_{\text{ind-exch}}^2$, $E_{\text{disp-exch}}^2$ contribute positively and hence, repulsively as it is expected for the phenomenon of exchange. Taking a look to the summed first and second order energy contributions E_{tot}^1 and E_{tot}^2 one can see that the second order energy is negative for all cases. In case of the unpolar argon dimer, this can be explained by the large contribution of the dispersion energy which is a second order quantity. In case of the water and uracil dimers, dispersion still gives a large part of the energy, but the induction energy is slightly larger for water and significantly larger for uracil which can be deduced to the polar nature of the latter dimers as compared to argon. Since the summed second order contributions are close to each other w.r.t the comparison between HF and PBE0, the

Table 1: Contributions to the binding energies of the argon, water and uracil dimers obtained by SAPT. Energies are given in E_h .

	E_{pol}^1	E_{exch}^1	E_{ind}^2	$E_{\text{ind-exch}}^2$	E_{disp}^2	$E_{\text{disp-exch}}^2$	E_{tot}^1	E_{tot}^2	$E_{\text{tot}}^1 + E_{\text{tot}}^2$
Ar ₂ /HF	-0.1195	0.4005	-0.1469	0.1442	-0.5018	0.0355	0.2811	-0.4692	-0.1881
Ar ₂ /PBE0	-0.1249	0.4120	-0.1544	0.1513	-0.5236	0.0382	0.2871	-0.4886	-0.2016
(Uracil) ₂ /HF	-26.8849	25.3701	-12.8279	6.2995	-8.7528	1.5528	-1.5147	-13.7284	-15.2431
(Uracil) ₂ /PBE0	-25.7862	29.4175	-15.6878	9.4262	-9.6500	1.9399	3.6314	-13.9717	-10.3403
(H ₂ O) ₂ /HF	-7.3830	5.4955	-2.3656	1.2402	-2.2502	0.3952	-1.8875	-2.9804	-4.8679
(H ₂ O) ₂ /PBE0	-7.0930	6.3003	-2.7487	1.6166	-2.4950	0.4730	-0.7927	-3.1542	-3.9469

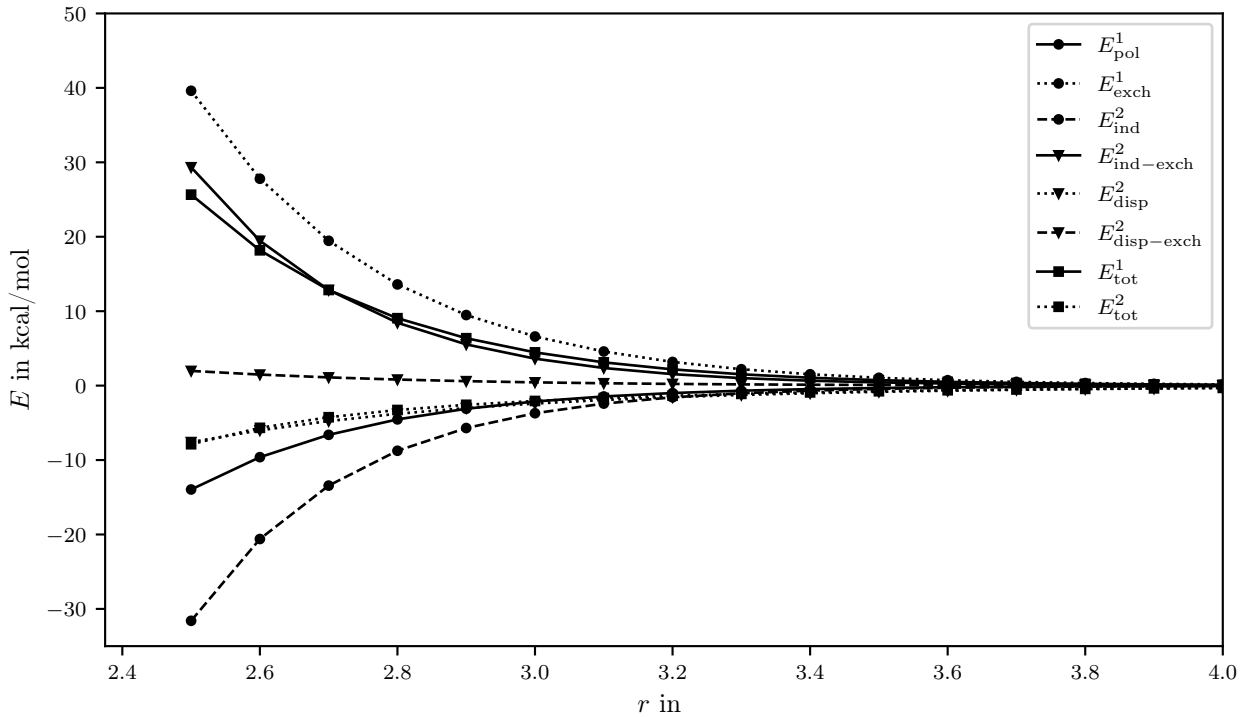


Figure 1: Distance-dependent partitioning of the noncovalent interactions in the argon dimer.

differences in the binding energy are produced by the differences in the summed first order energy contributions which are mainly caused by the first order exchange energy. The summed first order energies are positive in case of argon (missing dispersion as explained before). For water and uracil, they strongly differ between HF and PBE0 resulting even in opposite signs in case of uracil. The more repulsive nature of the DFT energy is deduced to the wrong PBE0 potential. Although it is asymptotically corrected, this correction is not sufficient and the potential still decays too fast.

The polarity of the molecules increases in the order argon < water < uracil leading to shorter distances between the monomers. Accordingly, the short-ranged exchange becomes more important and heavily contributes to the binding energy. Hence, the too repulsive DFT potential causes deviations as compared to the overbinding HF in the above-mentioned order.

1.2 Potential energy surface of the argon dimer

The potential energy surface of the argon dimer was computed between 2.5 and 4.0 Å on the HF-SAPT/aug-cc-pVTZ level of theory. The distance dependency of all contributions to the binding energy is displayed in Figure 1.

Overall, it can be observed that the contributions decay to zero with increasing monomer distance. Note that their convergence behavior is different and will be exemplary discussed below. First order polarization as well as second order induction and dispersion contribute attractively, whereas the mixed second order terms and the first order exchange energy contribute repulsively. The magnitude of the contributions at the equilibrium distance of 3.76 Å is shown in Table 1. At smaller distances, most of the contributions – except for $E_{\text{disp-exch}}$ – become very large.

The analytical distance dependencies of the first order exchange and second order dispersion energy are e^{-r} and r^{-6} , respectively as shown in Figure 2.

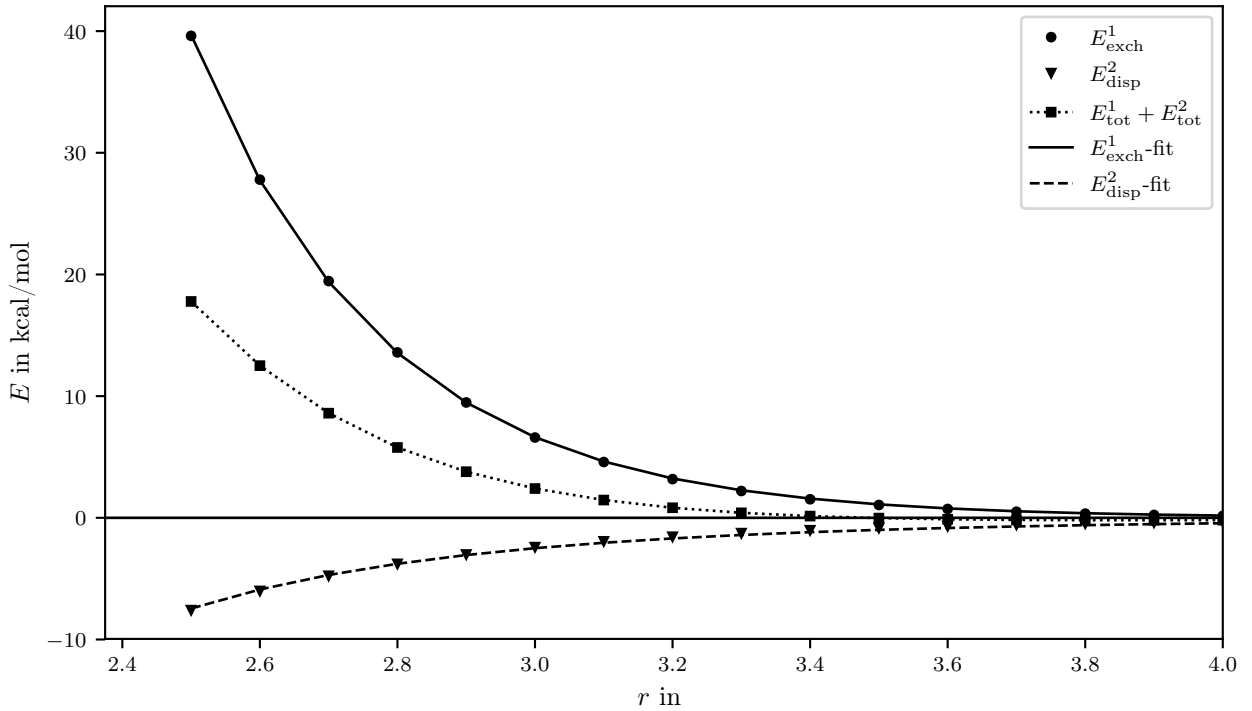


Figure 2: Distance-dependency of the first order exchange E_{exch}^1 and second order dispersion energy E_{disp}^2 and suitable fits (e^{-r} and r^{-6} , respectively) in the argon dimer.

2 Supermolecular Approaches

Reference binding energies of two weakly bound dimers were to be computed. Hence, energies of the water and argon monomer and dimer were computed on the MP2/aug-cc-pVTZ, MP2/aug-cc-pVQZ and CCSD(T)/aug-cc-pVTZ level of theory employing the TURBOMOLE^[8,9] program package and subsequently extrapolated to the basis set limit as explained below.

The binding energy of a system AB consisting out of two fragments A, B is (in the supermolecular approach) defined by the energy difference between the AB system E_{AB} and the (summed) fragments E_A , E_B :

$$E_{\text{bind}} = E_{AB} - (E_A + E_B) . \quad (2)$$

The total energy E_{tot} of an arbitrary system is composed of the SCF energy E_{SCF} and correlation energy E_{corr} . Aiming for high accuracy and facing the enormous computational effort of CCSD(T) calculations with large basis set (X^7 scaling w.r.t. the basis set size X), extrapolation techniques come into play. Knowing the convergence behavior of E_{SCF} and E_{corr} , w.r.t. X

$$E_{\text{SCF}}^{(\infty)} = E_{\text{SCF}}^{(X)} + A \cdot e^{-\alpha\sqrt{X}} \quad (3)$$

$$E_{\text{corr}}^{(\infty)} = E_{\text{corr}}^{(X)} + B \cdot X^{-\beta} \quad (4)$$

one can extrapolate the energies to the basis set limit (CBS) via

$$E_{\text{SCF}}^{(\text{CBS})} = \frac{E_{\text{SCF}}^{(X_1)} \cdot e^{\alpha\sqrt{X_1}} - E_{\text{SCF}}^{(X_2)} \cdot e^{\alpha\sqrt{X_2}}}{e^{\alpha\sqrt{X_1}} - e^{\alpha\sqrt{X_2}}} \quad (5)$$

Table 2: Hartree–Fock energies E_{RHF} , correlation energies E_{corr} and total energies E_{tot} (all in E_h) of the water and argon monomer and dimer. **XZ** refers to aug-cc-pV**XZ**.

(a) Energies of water.

	Monomer			Dimer		
	E_{RHF}	E_{corr}	E_{tot}	E_{RHF}	E_{corr}	E_{tot}
MP2/TZ	-76.060707	-0.268399	-76.329106	-152.126933	-0.539404	-152.666337
MP2/QZ	-76.066089	-0.285972	-76.352061	-152.137665	-0.574415	-152.712080
CCSD(T)/TZ	-76.060707	-0.281761	-76.342468	-152.126933	-0.566184	-152.693117

(b) Energies of argon.

	Monomer			Dimer		
	E_{RHF}	E_{corr}	E_{tot}	E_{RHF}	E_{corr}	E_{tot}
MP2/TZ	-526.813355	-0.210921	-527.024277	-1053.626321	-0.422740	-1054.049060
MP2/QZ	-526.816807	-0.232142	-527.048949	-1053.633199	-0.465215	-1054.098413
CCSD(T)/TZ	-526.813355	-0.235403	-527.048758	-1053.626321	-0.471625	-1054.097946

Table 3: Binding energies of the water and argon dimer in kcal/mol computed on different levels of theory and comparison to the experiment.

	HF/CBS	CCSD(T)/CBS	AC-PBE0-SAPT	Reference
(H ₂ O) ₂	-3.444	-4.967	-3.947	-4.94 ^[10]
Ar ₂	0.261	-0.290	-0.202	-0.285 ^[11]

$$E_{\text{corr}}^{(\text{CBS})} = \frac{E_{\text{corr}}^{(\text{X}_1)} \cdot \text{X}_1^\beta - E_{\text{corr}}^{(\text{X}_2)} \cdot \text{X}_2^\beta}{\text{X}_1^\beta - \text{X}_2^\beta} . \quad (6)$$

As can be seen from Equation 3 and Equation 4, SCF and correlation energy show a different convergence behavior enabling a separate extrapolation for both of them according to Equation 5 and Equation 6. The parameters α, β are basis set dependent and were optimized for the present case as $\alpha = 5.79$ and $\beta = 3.05$. To extrapolate CCSD(T) results to the basis set limit, the following formula can be applied:

$$E_{\text{CCSD(T)}}^{(\text{CBS})} \approx E_{\text{MP2}}^{(\text{CBS})} + (E_{\text{CCSD(T)}}^{(\text{X})} - E_{\text{MP2}}^{(\text{X})}) . \quad (7)$$

The results are given in Table 2. Extrapolations to the basis set limit were performed according to the given equations. The use of augmented basis sets is reasonable and recommended because the accurate descriptions of long-ranged interactions requires the inclusion of diffuse basis functions that extend far in space and functions with higher angular momentum. CCSD(T)/CBS results are almost equal to the reference data, as displayed in Table 3. HF is – although extrapolated to the basis set limit – far off the reference because there is per definition no dispersion included. Any kind of BSSE is very unlikely occur under the assumption that the extrapolation to the basis set limit is correct. AC-PBE0-SAPT yields results which are closer to the experiment but nevertheless not good. Improvement could be made by adding a dispersion correction to HF and/or using a better functional in SAPT.

3 Molecules in Solution

The equilibrium association free energy ΔG_a of a host-guest system (molecular tweezer with tetracyanoquinone) at room temperature in toluene was accessed by a supermolecular approach. There are different contributions to this quantity, namely the DFT Energy E_{tot} , the two- and three-body dispersion correction $E_{\text{D3}}^{\text{ATM}}$, the geometrical Counter-Poise correction energy E_{gCP} , the free energy correction in the rigid-rotor-harmonic-oscillator approximation $\Delta G_{\text{RRHO}}^{298}$ and the solvent free energy correction $\Delta \delta G_{\text{solv}}^{298}$:

$$\Delta G_a = E_{\text{tot}} + E_{\text{D3}}^{\text{ATM}} + E_{\text{gCP}} + \Delta G_{\text{RRHO}}^{298} + \Delta \delta G_{\text{solv}}^{298} . \quad (8)$$

E_{tot} and $E_{\text{D3}}^{\text{ATM}}$ were computed on a TPSS^[12]-D3^{ATM}^[13,14]/def2-TZVP^[15] level of theory using the TURBOMOLE program package. E_{gCP} was computed by the gcp^[16] program. The free energy corrections $\Delta G_{\text{RRHO}}^{298}$ were computed on the GFN2-xTB^[17]-level of theory based on the TPSS-D3^{ATM}/def2-TZVP geometries. The solvent free energy corrections $\Delta \delta G_{\text{solv}}^{298}$ were calculated by COSMO-RS model as implemented in TURBOMOLE.^[18] The process of interest can be summarized by the following equation:



Accordingly, any energy contribution Δ_i from Equation 8 can be expressed as

$$\Delta_i = E_i^{\text{Complex}} - (E_i^{\text{Host}} + E_i^{\text{Guest}}) . \quad (10)$$

The results are given in Table 4 and add up to $\Delta G_a = -1.41$ kcal/mol, which strongly deviates from the experimental result of $\Delta G_a^{\text{exp}} = -4.50$ kcal/mol. Although this error is remarkable, note that the accurate description of the investigated process is rather demanding since the host-guest system is dominated by noncovalent interactions. It is quite favorable that the calculations at least yielded a bound host-guest system.

Improvements could be made by choosing more accurate methods to compute the different contributions, e.g. by using a (double) hybrid functional for the electronic energies and vibrational frequencies, trying to correct the (usually) overcompensating geometrical Counter-Poise

Table 4: Contributions to the equilibrium association free energy of the host-guest system. Energies are given in E_{h} .

System	E_{tot}	E_{disp}	E_{gCP}	$\Delta G_{\text{RRHO}}^{298}$	$\Delta \delta G_{\text{solv}}^{298}$
host	-1619.355877	-0.145975	0.037984	0.526756	-0.045041
guest	-678.950769	-0.035501	0.007677	0.082988	-0.023998
complex	-2298.299259	-0.239366	0.047508	0.633091	-0.045983
Δ	0.007387	-0.057890	0.001848	0.023347	0.023056

correction or use an explicit solvation model. These suggestions, especially concerning the frequency calculation, would of course come along with a dramatically increased computational cost.

4 Organic Solids

The sublimation enthalpy ΔH_{sub} of an organic urea crystal at room temperature was computed. First, electronic energies of both phases were computed on the TPSS-D3^{ATM}/600 eV level of theory using the VASP^[19–21] program package and a k grid of $\approx 1/35 a_0^{-1}$. After that, electronic energies and free energy corrections were computed at the semiempirical DFTB3^[22]-D3 level of theory and the same k grid as mentioned before. To access the frequencies, a phonon calculation and the Γ -point with a 3x3x3 supercell was performed. A supercell is necessary to include low energetic modes of the solid. The supercell was enlarged until the contributions were converged within 1 kcal/mol.

The sublimation enthalpy defined as the difference between the enthalpies of the two phases H_{gas} , H_{solid} which themselves can be split up into different contributions

$$\Delta H_{\text{sub}} = H_{\text{gas}} - H_{\text{solid}} \quad (11)$$

$$H^i = E_{\text{el}}^i + E_{\text{trans}}^i + E_{\text{rot}}^i + E_{\text{vib}}^i + pV, \quad (12)$$

where the E^i denote the electronic, translational, rotational and vibrational energy contributions, respectively. pV is the volume work. The vibrational energy is treated in the harmonic approximation and therefore consists of a constant part – the zero-point vibrational energy ZPVE – and a temperature dependent part $E_{\text{vib}}^{\text{DFTB}}$. The translational and rotational energy contributions are derived from the equipartition theorem (under the assumption of an ideal gas),

$$E_{\text{trans}} = E_{\text{rot}} = \frac{3}{2}RT, \quad (13)$$

where R , T denote the ideal gas constant and temperature, respectively.

The results are given in Table 5. Taking a closer look to the TPSS-D3^{ATM}/600 eV energy, it is revealed that the dispersion energy itself contributes to the electronic energy by -3.39 kcal/mol and -13.53 kcal/mol for the gaseous and solid state, respectively. The influence is small for the gas phase (around 0.25 %) but significant for the solid state (more than 2.0 %). This becomes especially important when calculating energy differences – as in the present case. Hence, using a dispersion correction is always recommended. Note that the computational effort of adding a dispersion correction is negligible.

Summing up all different contributions for DFTB and TPSS, sublimation enthalpies of $\Delta H_{\text{sub}}^{\text{TPSS}} = 25.39$ kcal/mol and $\Delta H_{\text{sub}}^{\text{DFTB}} = 26.68$ kcal/mol are yielded. Compared to the experimental value of $\Delta H_{\text{sub}}^{\text{exp}} = 22.42$ kcal/mol, there are deviations of 16 % and 19 % for TPSS and DFTB, respectively. DFT energies are computed under usage of the Born–Oppenheimer approximation. As a consequence of this approximation, the Hamiltonian is reduced to an electronic Hamiltonian which accounts for the electronic energy, exclusively. Thermal energy

Table 5: Contributions to the sublimation enthalpy of urea. Energies are given in kcal/mol.

	$E_{\text{el}}^{\text{TPSS}}$	$E_{\text{D3}}^{\text{TPSS}}$	$E_{\text{el}}^{\text{DFTB}}$	ZPVE	E_{trans}	E_{rot}	$E_{\text{vib}}^{\text{DFTB}}$	pV	H^{TPSS}	H^{DFTB}
solid	-1293.40	-13.53	-7150.34	38.81	0.00	0.00	3.29	0.00	-1306.90	-7108.24
gas	-1278.15	-3.39	-7123.36	37.73	0.89	0.89	2.23	0.06	-1281.50	-7081.56

contributions arise from the movement of the nuclei (translation, rotation, vibration) that are explicitly neglected. Thus, no thermal effects are included. Furthermore, other approximations were employed as mentioned before: The assumption of urea as an ideal gas and the assumption of the vibrations to be purely harmonic. At a first glance, these assumptions are well-founded and enormously speed up calculations. Taking a closer look, it has to be noted that they are not necessarily reasonable and may lead to errors. Employing a more realistic model for the urea gas and adding anharmonicities would improve the accuracy as well as the computational cost of this calculation.

Literature

- [1] B. Jeziorski, R. Moszynski, K. Szalewicz, *Chem. Rev.* **1994**, *94*, 1887–1930.
- [2] H.-J. Werner, P. J. Knowles, G. Knizia, F. R. Manby, M. Schütz, et al., MOLPRO, version 2012.1, a package of ab initio programs, see <http://www.molpro.net>, Cardiff, UK, **2012**.
- [3] R. A. Kendall, T. H. Dunning, R. J. Harrison, *J. Chem. Phys.* **1992**, *96*, 6796–6806.
- [4] D. E. Woon, T. H. Dunning, *J. Chem. Phys.* **1993**, *98*, 1358–1371.
- [5] C. Adamo, V. Barone, *J. Chem. Phys.* **1999**, *110*, 6158–6170.
- [6] NIST Chemistry WebBook, <https://webbook.nist.gov/chemistry/>.
- [7] A. Hesselmann, G. Jansen, M. Schuetz, *The Journal of chemical physics* **2005**, *122*, 014103.
- [8] TURBOMOLE V7.4.1 2019, a development of University of Karlsruhe and Forschungszentrum Karlsruhe GmbH, 1989-2007, TURBOMOLE GmbH, since 2007; available from <https://www.turbomole.org>.
- [9] S. G. Balasubramani, G. P. Chen, S. Coriani, M. Diedenhofen, M. S. Frank, Y. J. Franzke, F. Furche, R. Grotjahn, M. E. Harding, C. Hättig, A. Hellweg, B. Helmich-Paris, C. Holzer, U. Huniar, M. Kaupp, A. M. Khah, S. K. Khani, T. Müller, F. Mack, B. D. Nguyen, S. M. Parker, E. Perlt, D. Rappoport, K. Reiter, S. Roy, M. Rückert, G. Schmitz, M. Sierka, E. Tapavicza, D. P. Tew, C. van Wüllen, V. K. Voora, F. Weigend, A. Wodyński, J. M. Yu, *J. Chem. Phys.* **2020**, *152*, 184107.
- [10] M. Schütz, S. Brdarski, P.-O. Widmark, R. Lindh, G. Karlström, *The Journal of chemical physics* **1997**, *107*, 4597–4605.
- [11] R. Podesszwa, K. Szalewicz, *Chemical physics letters* **2005**, *412*, 488–493.
- [12] J. Tao, J. P. Perdew, V. N. Staroverov, G. E. Scuseria, *Phys. Rev. Lett.* **2003**, *91*, 146401.
- [13] S. Grimme, J. Antony, S. Ehrlich, H. Krieg, *J. Chem. Phys.* **2010**, *132*, 154104.
- [14] S. Grimme, S. Ehrlich, L. Goerigk, *J. Comput. Chem.* **2011**, *32*, 1456–1465.
- [15] F. Weigend, R. Ahlrichs, *Phys. Chem. Chem. Phys.* **2005**, *7*, 3297–3305.
- [16] H. Kruse, S. Grimme, *J. Chem. Phys.* **2012**, *136*, 154101.
- [17] C. Bannwarth, S. Ehlert, S. Grimme, *J. Chem. Theory Comput.* **2019**, *15*, 1652–1671.
- [18] F. Eckert, A. Klamt, *COSMOtherm, Version C30-1601 (revision 2299), release 16.01*, COSMOlogic GmbH & Co. KG, Leverkusen (Germany), **2016**.
- [19] R. A. Kendall, T. H. Dunning, R. J. Harrison, *J. Chem. Phys.* **1992**, *96*, 6796–6806.
- [20] G. Kresse, J. Furthmüller, *Comput. Mater. Sci.* **1996**, *6*, 15–50.
- [21] G. Kresse, J. Furthmüller, *Phys. Rev. B* **1996**, *54*, 11169–11186.

- [22] M. Gaus, Q. Cui, M. Elstner, *J. Chem. Theory Comput.* **2011**, 7, DFTB3, 931–948.